

Detection of nanocrystallinity by X-ray absorption spectroscopy in thin film transition metal/rare-earth atom, elemental and complex oxides

L.F. Edge^a, D.G. Schlom^a, S. Stemmer^b, G. Lucovsky^{c,*}, J. Luning^d

^aDepartment of Materials Science, Pennsylvania State University, State College, PA, USA

^bDepartment of Materials Science, University of California at Santa Barbara, Santa Barbara, CA, USA

^cDepartment of Physics, Raleigh, North Carolina State University, NC, USA

^dStanford Synchrotron Radiation Labs, Stanford University, Menlo Park, CA, USA

Abstract

Nanocrystallinity has been detected in the X-ray absorption spectra of transition metal and rare-earth oxides by (i) removal of d-state degeneracies in the (a) Ti and Sc L₃ spectra of TiO₂ and LaScO₃, respectively, and (b) O K₁ spectra of Zr(Hf)O₂, Y₂O₃, LaScO₃ and LaAlO₃, and by the (ii) detection of the O-atom vacancy in the O K₁ edge ZrO₂–Y₂O₃ alloys. Spectroscopic detection is more sensitive than X-ray diffraction with a limit of ~2 nm as compared to >5 nm. Other example includes detection of ZrO₂ nanocrystallinity in phase-separated Zr(Hf) silicate alloys.

© 2006 Elsevier Ltd. All rights reserved.

PACS: 71.17.Ej; 73.63.Bd; 78.20.Ci; 78.70.Dm

Keywords: X-ray absorption spectra; Nanocrystallinity; X-ray absorption spectroscopy; Elemental oxides; Complex oxides; Jahn–Teller splittings; O-atom vacancies

1. Introduction

There has been considerable interest in the bonding morphology of elemental and complex transition metal (TM) and lanthanide rare-earth (RE) oxides, in particular in distinguishing between non-crystalline and amorphous thin films, including those that are nanocrystalline with grain sizes as small as 2 nm. This paper includes spectroscopic approaches, primarily X-ray absorption spectroscopy (XAS), to reveal electronic structure unique to nanocrystalline solids. These studies demonstrate that this spectroscopic approach is sig-

nificantly more sensitive than conventional X-ray diffraction (XRD), but comparable to lattice imaging using high-resolution transmission electron microscopy (HRTEM).

2. Experimental procedures

The thin film TM/RE complex oxides were prepared by reactive evaporation. These oxide films are nanocrystalline as-deposited with grain sizes increasing with high-temperature annealing in inert ambients such as Ar. XAS measurements were performed at the Stanford Synchrotron Research Laboratory (SSRL) on as-deposited films, and films annealed inert at temperatures up to

*Corresponding author.

E-mail address: lucovsky@ncsu.edu (G. Lucovsky).

1000 °C. Other spectroscopic and characterization measurements were made on state-of-the-art laboratory instruments.

3. Experimental results

Jahn–Teller (J–T) term splittings have been detected by XAS in group IVB TM oxides in the $L_{2,3}$ edge in TiO_2 in Fig. 1(a), and by differentiation of features in the O K_1 edges of ZrO_2 in Fig. 1(b) and HfO_2 . Core hole lifetimes of the 3p, and 4p states are too short due to relativistic effects for atomic numbers, Z , in excess of 40, and spectral line-widths of M_3 and N_3 transitions are too broad, $>2\text{ eV}$, to resolve J–T term splittings in ZrO_2 , Y_2O_3 and HfO_2 (Lucovsky et al., 2005). Consistent with longer O 1s core hole lifetimes, 4d and 5d state degeneracy removal has been demonstrated in differentiated O K_1 spectra, as in Fig. 1(a) for ZrO_2 . J–T splittings in Ti d-states are not resolved in the O K_1 edge of TiO_2 .

For complex oxides such as $LaScO_3$ d-state splittings are observed directly in the Sc L_3 spectrum and the O K_1 edge. The only significant differences in Sc L_3 and O K_1 spectra for $LaScO_3$ samples annealed at different temperatures is the width of the spectral features, and not the degeneracy removal. The full-widths at half-maximum of the features in the Sc L_3 spectra are essentially the same in as-deposited films, and those annealed at 700 °C, but decrease by approximately 50% upon annealing to 1000 °C. Sc L_3 spectra in Fig. 2(a) and (b) indicate these different spectral line-widths. This establishes $LaScO_3$ films are nanocrystalline on deposition. In marked contrast, crystallinity is detected by

XRD only after annealing to 800 °C, consistent with HRTEM studies that indicate grain sizes of the order of 2 nm in the as-deposited films.

Similar considerations apply to $LaAlO_3$: J–T term splittings associated with Al 3p states are easily detected in as-deposited O K_1 edge spectra, whereas XRD detection of crystallinity is detected only after annealing at about 800 °C. Nanocrystallinity is also evident in Zr titanate $Ti_{1-x}Zr_xO_2$ and O K_1 spectra at the compound compositions: $ZrTiO_2$ and $ZrTi_2O_6$ (Hom et al., 2001). In contrast in non-stoichiometric compositions, $HfTiO_4$ and Zr_2TiO_6 , Ti L_3 spectra indicate nanocrystallinity of the TiO_2 alloy, but absence of J–T term splittings in both Hf and Zr O K_1 edges indicates a more significantly disordered nanostructure for HfO_2 and ZrO_2 constituents.

Another example of nanocrystallinity detection is displayed in Fig. 3(a), which includes O K_1 edge spectra for ZrO_2 annealed to 500 and 800 °C, as well as insert that indicates a weaker feature below the band edge $4d_{3/2}$ state absorption for the sample annealed at 800 °C. This weak feature has been assigned to a transition from the O K_1 (1s) core state to an O-vacancy. This assignment is supported by the O K_1 edge spectrum in Fig. 3(b) for a Y_2O_3 – ZrO_2 alloy with $\sim 18\%$ Y_2O_3 . The cubic structure in these low Y_2O_3 alloys is stabilized by O-atom vacancies. It is significant to note that 4d-state degeneracy removal in ZrO_2 is evident at both annealing temperatures by numerical differentiation of the respective spectra, but that the weaker feature, also associated with crystallinity is not detected until the sample is annealed to 800 °C, here assigned to larger grain size.

The final example of nanocrystallinity detection is for Zr silicate alloys, $(ZrO_2)_x(SiO_2)_{1-x}$, and representative

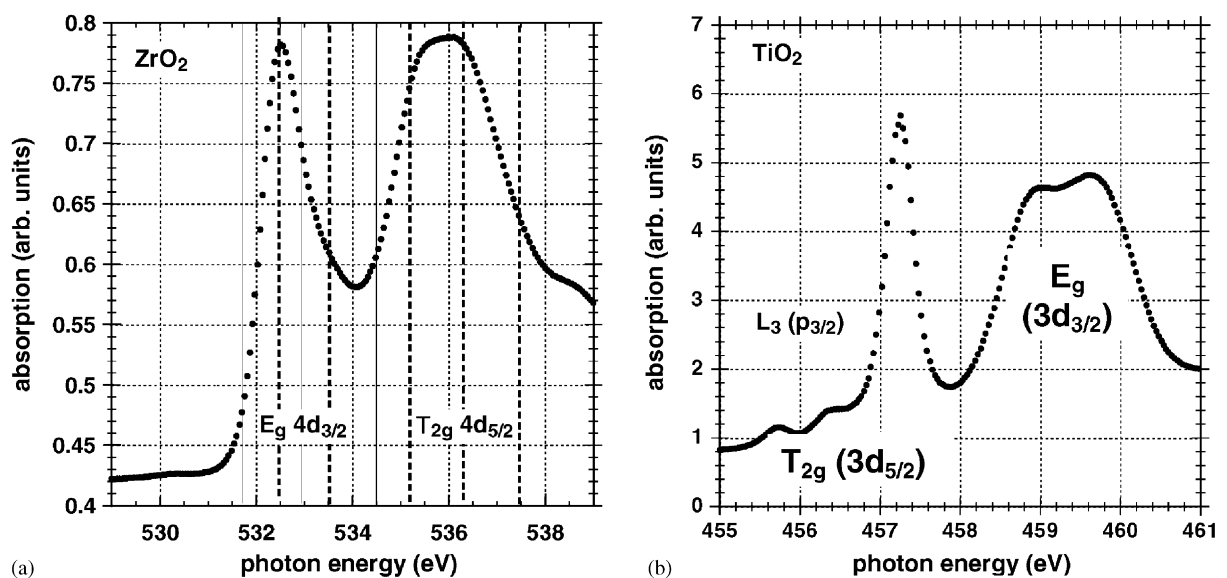


Fig. 1. d-state degeneracy removal confirms nanocrystallinity: (a) O K_1 edge in ZrO_2 , and (b) Ti L_3 edge in TiO_2 .

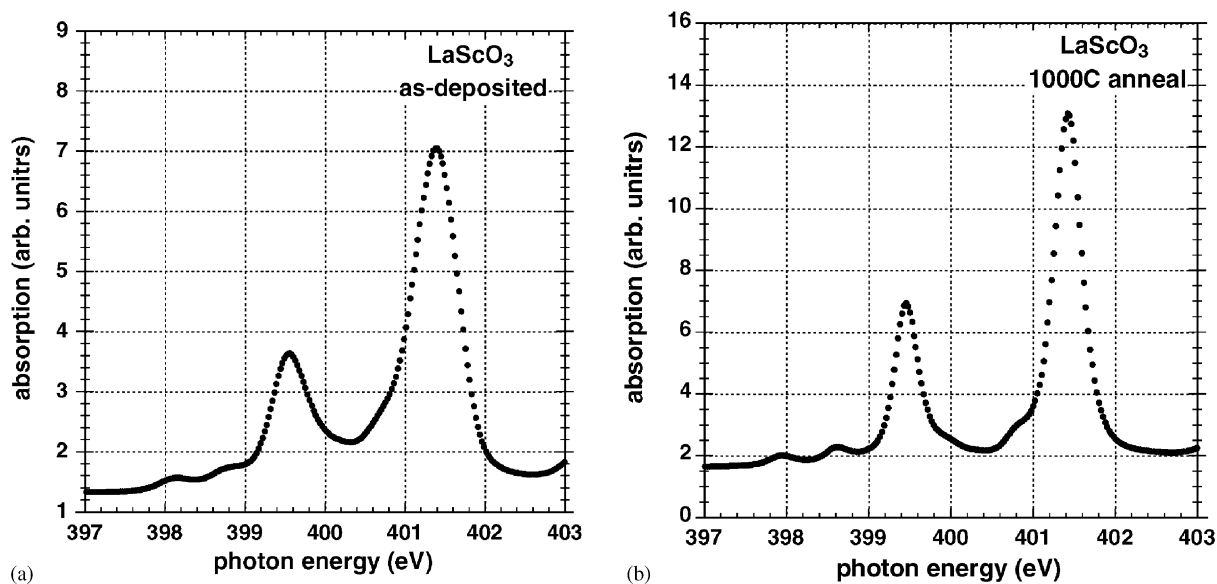


Fig. 2. d-state degeneracy removal in Sc L_3 edge in LaScO_3 confirms nanocrystallinity: (a) as-deposited, (b) after 1000°C anneal.

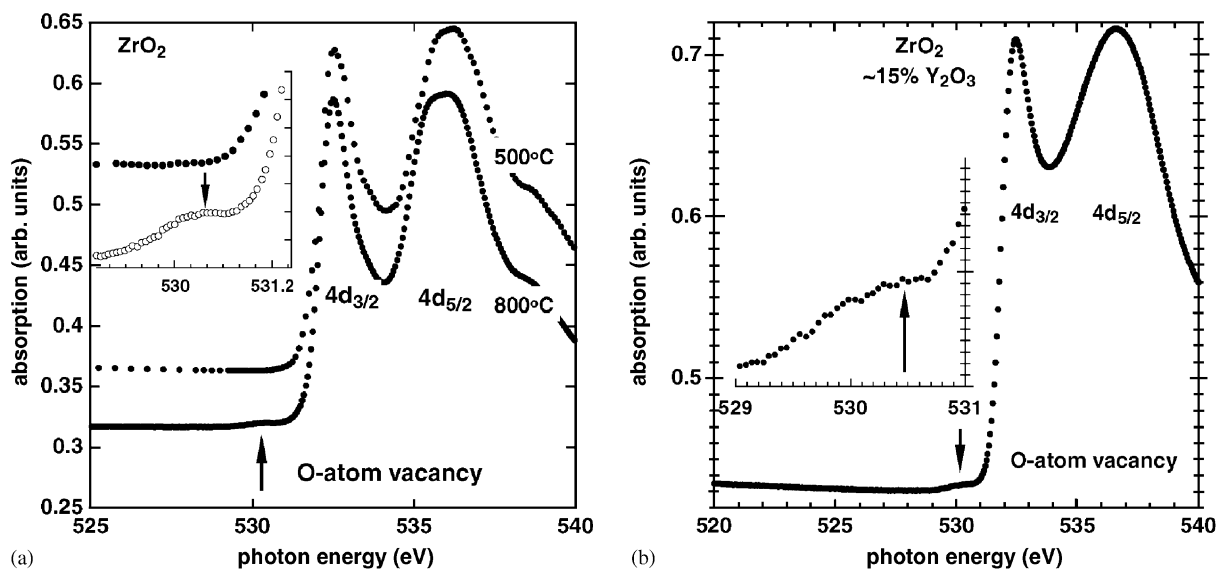


Fig. 3. O K_1 edge spectra of (a) ZrO_2 and (b) a Y_2O_3 - ZrO_2 alloy. Each spectrum indicates vacancy absorption confirming nanocrystallinity.

spectra are included in Fig. 4. The spectral changes are between the first 4d-state feature in the as-deposited and 900°C annealed films with $x\sim 0.3$ and $x\sim 0.6$ are consistent with a non-crystalline film as-deposited film, and nanocrystalline film after the anneal. In this instance, and for films with $x>0.5$, crystallinity is readily detectable by XRD. However, similar differences between as-deposited and annealed films have been detected by XAS in films with $x\sim 0.2$ – 0.3 , where nanocrystallinity was not detected by XRD, but

confirmed by extend X-ray absorption fine structure (EXAFS) and HRTEM imaging.

4. Discussion

The complete removal of d-state degeneracies in either L_3 , $3p_{3/2}$ to empty 4d-state transitions, or in O K_1 edge or differentiated O K_1 edge transitions that originate in the O 1s core state, and terminate in anti-bonding O 2p

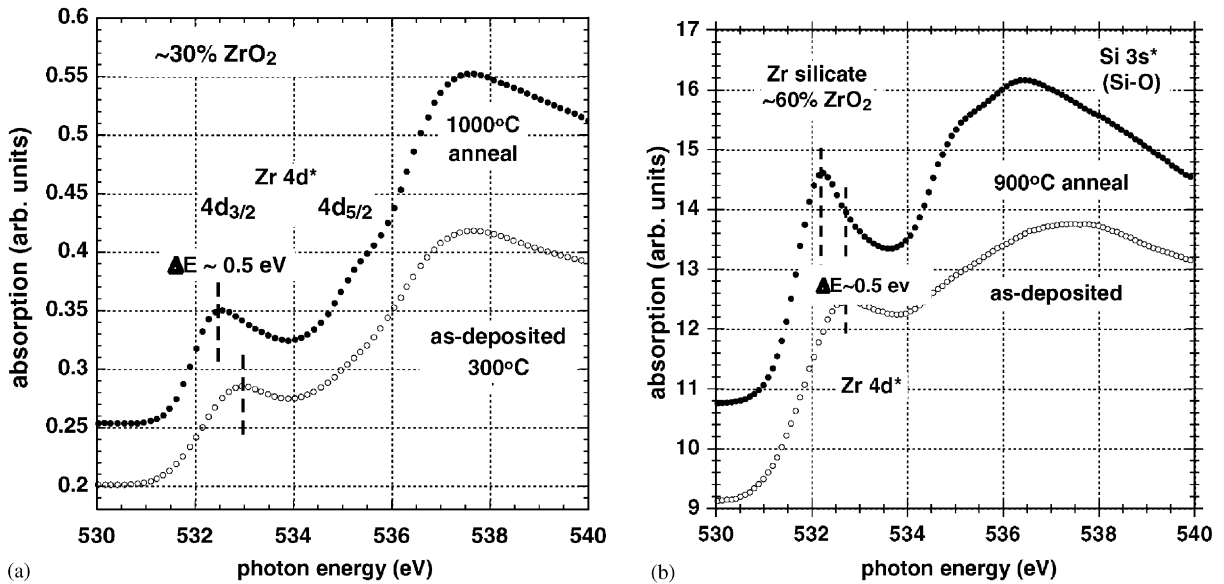


Fig. 4. O K₁ edge spectra for Zr silicate alloys with ~30% of ZrO₂ in (a) and ~68% ZrO₂ in (b). These alloys are non-crystalline as as-deposited at 30 °C, but display J–T term splittings after a 900 °C anneal nanocrystallinity of the ZrO₂ phase.

states that are mixed with TM/RE d- and s-states, is only possible in oxides with a sufficient degree of nanocrystallinity, approximately 2 nm. This scale order is sufficient for providing coherent bonding interactions that extend to at least 2nd and 3rd neighbor shells of first row TM/RE atoms such as Ti and Sc. d-state degeneracy removal cannot be detected in the M₃ or N₃ levels of TM/RE atoms, due to core-hole lifetime effects. These are sufficiently short for atomic numbers, $Z > 40$, for absorption line-widths for Y and Zr M₃ transitions to be greater than 2 eV, and hence greater than anticipated J–T term splittings where they are typically less than or equal to about 1 eV.

Two representative complex oxides, LaScO₃ and LaAlO₃, display J–T term splittings in O K₁ spectra, that are associated, respectively, with Sc 3d and Al 3p states. This illustrates another interesting aspect of the J–T, namely that this effect is not restricted to d-state atoms, but can occur in atoms with partially occupied p-states as well. By correlating band edge features in photoconductivity, PC, in LaScO₃ with L₃ and O K₁ edge J–T splittings this spectrum also provides detection of nanocrystallinity below the XRD limit. A similar situation prevails for LaAlO₃, where band edge PC features correlate with O K₁ J–T features as well.

A second and interesting manifestation of nanocrystallinity derives from vacancy incorporation in TM/RE elemental and complex oxides. These materials are typically very good to excellent ionic conductors, e.g., ZrO₂. The ZrO₂ O K₁ spectra in Fig. 3 display 4d-state degeneracy removal by differentiation so that films annealed at 500 and 800 °C are nanocrystalline. How-

ever, only the spectrum of the film annealed at 800 °C displays detectable absorption associated with transitions from the O 1s core state to O-atom vacancies within the band-gap of ZrO₂. This is interpreted as in terms of the marked increase in grain growth kinetics that typically occurs at about 800–900 °C in TM/RE elemental and complex oxides, and TM silicates as well.

A final example of nanocrystallinity detection has been demonstrated for Zr silicate alloys. In this instance, XAS, as well as infrared absorption, EXAFS and HRTEM imaging have all been used to detect nanocrystalline grains below the limit of XRD detection, i.e., <3 nm.

5. Conclusions

Nanocrystallinity at scale of 2 nm has been detected in X-ray absorption spectra of TM and lanthanide RE elemental and complex oxides by (i) the removal of d-state degeneracies in the (a) Ti and Sc L₃ spectra of TiO₂, and LaScO₃, respectively, and (b) O K₁ spectra of Zr(Hf)O₂, Y₂O₃, LaScO₃ and LaAlO₃, and by (ii) the detection O K₁ core level to O-atom vacancy level absorptions in ZrO₂, Y₂O₃, and ZrO₂–Y₂O₃ alloys. Spectroscopic detection is more sensitive than X-ray diffraction (XRD) with a limit of ~2 nm as compared to >5 nm XRD limitation. Similar considerations apply to detection of Zr(Hf)O₂ nanocrystallinity in phase-separated Zr(Hf) silicate alloys.

This research has established X-ray absorption spectroscopy (XAS), in particular X-ray absorption

near-edge spectroscopy or XANES, as a fast and reliable way to determine whether a thin film is nanocrystalline or amorphous. It makes it unnecessary to refer to films as XRD amorphous, wherein this designation does provide any useful information relative to nanocrystallinity at scale below about 5 nm, and therefore relative to electronically active defect states at either internal grain boundaries, or at O-atom vacancies associated with that scale of grain sizes.

Analysis of XAS spectra as a function of processing temperatures provides information relative to (i) the kinetics of solid crystal growth, as demonstrated for LaScO_3 , (ii) the chemical phase separation of Zr and Hf silicate alloys, and (iii) the formation of O-atom vacancies in elemental TM oxides. Preliminary results for LaScO_3 and Zr silicate alloys indicate that the information provided by the XAS studies is consistent with other measurements that reflect changes in grain size and/or chemical phase separation and crystallization.

Acknowledgements

This work was supported by ONR, DOE and SRC.

References

- Hom, B.K., Stevens, R., Woodfield, B.F., Boerio-Goatesa, J., Putnam, R.L., Helean, K.B., Alexandra, N., 2001. The thermodynamics of formation, molar heat capacity, and thermodynamic functions of ZrTiO_4 . *J. Chem. Thermodyn.* 33, 165–178.
- Lucovsky, G., Fulton, C.C., Zhang, Y., Zou, Y., Luning, J., Edge, L.F., Whitten, J.L., Nemanich, R.J., Ade, H., Schlom, D.G., Afanaseiv, V.V., Stesmans, A., Zollner, S., Triyoso, D., Rogers, B.R., 2005. Conduction band-edge States associated with the removal of d-state degeneracies by the Jahn–Teller effect. *IEEE Trans. Device Mater. Reliab.* 5, 65–83.